

Phase diagram of the square-lattice model with 1*q* and 2*q* incommensurate modulations

K. Parlinski

Institute of Nuclear Physics, ul. Radzikowskiego 152, 31-342 Cracow, Poland

(Received 15 September 1992)

A two-dimensional square-lattice model of particles with displacive degrees of freedom and interacting via a potential with harmonic and anharmonic fourth-order terms, one local and the second having the character of the three-body forces, has been considered. The calculated phase diagrams, characterized by the wave vectors along the $[k, 0]$, $[\frac{1}{2}, k]$, and $[k, k]$ directions, possess incommensurate and commensurate one-dimensional stripe 1*q* and two-dimensional 2*q* phases. The stable 2*q* modulated phases, which look like superpositions of two stripe phases, occur along the $[k, 0]$ and $[\frac{1}{2}, k]$ directions, and close to the $(\frac{1}{2}, 0)$ point of the reciprocal lattice, provided the magnitude of the three-body anharmonic potential exceeds a critical value.

I. INTRODUCTION

Crystals with incommensurate phases have long been a subject of extensive experimental¹ and theoretical studies in recent years.² Experimentally, it has been found that the majority of incommensurate phases occur in crystals with frame symmetry being orthorhombic, and that the modulation is one dimensional (1*q*) and propagates as a rule along a high-symmetry lattice direction. A two-dimensional incommensurate modulation (2*q*), which arises as a result of superposition of two static modulated waves, propagating along two different, but equivalent directions, occurs rather seldom. One example of it is known in tetragonal crystal of barium sodium niobate, Ba₂NaNb₂O₁₅.³⁻⁵ The normal phase of it is tetragonal with point symmetry 4*mm*. Below about 300 °C, a 2*q* modulated phase appears with satellites at the wave vectors $\mathbf{k} = \frac{1+\delta}{4}(\mathbf{a}^* + \mathbf{b}^*) + \frac{1}{2}\mathbf{c}^*$ and equivalent, where $\delta \sim 0.12 - 0.08$. Lowering further the temperature, the crystal first transforms to a stripe 1*q* phase, later to a lock-in phase at the wave vector $\mathbf{k} = \frac{1}{4}(\mathbf{a}^* + \mathbf{b}^*) + \frac{1}{2}\mathbf{c}^*$.

A special type of 2*q* modulation has been reported for the fcc based Cu_{0.78}Pd_{0.22} alloy.⁶⁻⁸ The system, below the disordered phase at 484 °C, exhibits a kind of 2*q* modulation with superimposed waves propagating along *a* and *c* cubic axes. However, the wave vectors of two waves are slightly different, hence, they do not belong to the same irreducible star. Consequently, this 2*q* modulated phase is not a conventional 2*q* phase, because it does not arise from condensation of a single irreducible star.

In hexagonal crystals a multidimensional incommensurate modulation, namely, the 3*q* modulation, has been found in a few cases. The best examples are quartz,^{9,10} AlPO₄,¹¹ and the charge-density-wave material 2H-TaSe₂.^{12,13}

A two-dimensional 2*q* pattern of convective rolls in an anisotropic liquid crystal similar to 2*q* modulation in incommensurate systems has also been observed.¹⁴

Up to now only Ising type models on a square lat-

tice with 2*q* phases have been considered. To that class belongs the lattice gas model¹⁵ with three-body forces, considered in relation to atoms and molecules adsorbed at the surface, the Ising model with up to third-nearest-neighbor couplings,¹⁶ and BNNI (biaxial next-nearest-neighbor Ising) model.¹⁷ The phase diagrams of the mentioned models have mainly commensurate phases of 1*q* and 2*q* types.

In this paper we propose a displacive model on a two-dimensional square lattice, which possesses stable incommensurate and commensurate phases of 1*q* and 2*q* types. The particles of the model are coupled by harmonic and fourth-order anharmonic forces. The harmonic forces decide whether the modulation is directed along $[k, 0]$, $[\frac{1}{2}, k]$, or $[k, k]$ lines of reciprocal lattice. The local anharmonic term stabilizes the system. Another anharmonic term, having a character of three-body forces, is entirely responsible for the appearance of the 2*q* modulated phase, stable along $[k, 0]$ and $[\frac{1}{2}, \frac{1}{2} - k]$ lines, provided $\frac{1}{4} \leq k \leq \frac{1}{2}$, and the strength of the three-body fourth-order anharmonic term exceeds a critical value.

The scope of the paper is the following. In Sec. II we define the square-lattice model and its properties. Schematic phase boundaries of the phase diagram are derived in Sec. III. Sec. IV summarizes the numerical scheme used to calculate the detailed phase diagrams for a few sets of potential parameters, which are referred to later in Sec. V. Final remarks close the paper.

II. MODEL

The model is a simple two-dimensional square lattice with one particle per unit cell, Fig. 1(a). Each particle has one degree of freedom which is a displacement $z_{j,l}$ in direction perpendicular to the plane of the model. Each particle is placed in the local anharmonic potential and interacts via harmonic forces with the first, second, and third nearest neighbors and via three-body fourth-order anharmonic potential within the nearest neighbors. The potential energy is written as

$$V = V^{(2)} + V^{(4)}, \quad (1a)$$

$$V^{(2)} = \frac{1}{2} \sum_{j,l} \{ Az_{j,l}^2 + Bz_{j,l}(z_{j+1,l} + z_{j-1,l} + z_{j,l+1} + z_{j,l-1}) + Cz_{j,l}(z_{j+1,l+1} + z_{j-1,l+1} + z_{j+1,l-1} + z_{j-1,l-1}) + z_{j,l}(z_{j+2,l} + z_{j-2,l} + z_{j,l+2} + z_{j,l-2}) \}, \quad (1b)$$

$$V^{(4)} = \frac{1}{2} \sum_{j,l} \{ z_{j,l}^4 + Hz_{j,l}^2(z_{j+1,l}z_{j,l+1} + z_{j,l+1}z_{j-1,l} + z_{j-1,l}z_{j,l-1} + z_{j,l-1}z_{j+1,l}) \}, \quad (1c)$$

with three independent parameters A, B, C in harmonic and one H in anharmonic terms. This form of the potential energy is quite general, although the coefficients in the harmonic term between second nearest neighbors and the coefficient in the local fourth-order anharmonic term are set to 1. It can always be done by choosing the displacement and potential energy units.¹⁸ We have disregarded other types of anharmonic terms since they are less promising in producing a stable $2q$ modulated phase.

The potential energy, Eqs. (1a)–(1c), could be rewritten in reciprocal space variables by applying the usual transformation to normal modes $Q_{\mathbf{k}}$,

$$z_{j,l} = \sum_{\mathbf{k}} Q_{\mathbf{k}} \exp(-2\pi i \mathbf{k} \cdot \mathbf{R}_{j,l}), \quad (2)$$

where $\mathbf{R}_{j,l} = j\mathbf{a} + l\mathbf{b}$ is the position vector of the (j, l) particle, $\mathbf{k} = k_x\mathbf{a}^* + k_y\mathbf{b}^*$ represents the wave vector, and \mathbf{a}, \mathbf{b} and $\mathbf{a}^*, \mathbf{b}^*$ are the unit vectors of the direct and reciprocal lattices, respectively, Fig. 1.

The potential energy, Eqs. (1a)–(1c), has a peculiar symmetry. Substituting each displacement by

$$z_{j,l} \rightarrow (-1)^{j+l} z_{j,l} \quad (3)$$

and changing simultaneously the sign of B coefficient

$$B \rightarrow -B \quad (4)$$

one finds the identical potential energy. Hence, the ground state energies of the configurations characterized by the wave vectors $\mathbf{k} = (0, 0)$ and $(\frac{1}{2}, \frac{1}{2})$ are the same, provided B has simultaneously changed the sign to $-B$. In this sense ($B \rightarrow B$) the two modulated configurations can be mapped to each other through the relation

$$(k_x, k_y) \rightarrow (\frac{1}{2} - k_x, \frac{1}{2} - k_y). \quad (5)$$

In particular, the ground-state energies of the modulated phases along $(k, 0)$ and $(\frac{1}{2} - k, \frac{1}{2})$ directions are the same

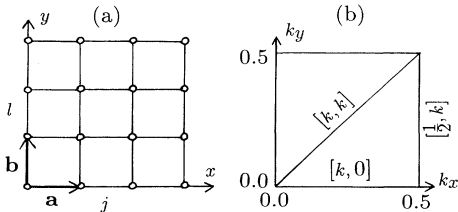


FIG. 1. The square-lattice model (a) and the reciprocal space of the model (b).

if $B < 0$ and $B > 0$, respectively.

Using Eq. (2), the harmonic part of the potential energy, Eq. (1b) becomes

$$V^{(2)} = \frac{1}{2} \sum_{\mathbf{k}} \omega^2(\mathbf{k}) Q_{\mathbf{k}} Q_{-\mathbf{k}}, \quad (6)$$

with the dispersion curve

$$\begin{aligned} \omega^2(k_x, k_y) = & A + 2B [\cos 2\pi k_x + \cos 2\pi k_y] \\ & + 2C [\cos 2\pi(k_x + k_y) + \cos 2\pi(k_x - k_y)] \\ & + 2 [\cos 4\pi k_x + \cos 4\pi k_y]. \end{aligned} \quad (7)$$

The dispersion curve, Eq. (7), is a single branch with non-zero value at the Brillouin zone center. Its surface has a fourfold symmetry. When negative, the minimum of the dispersion curve $\omega_{\min}^2(\mathbf{k})$ describes the wave vector and the direction of the static modulation. The simple form of the potential energy allows us to produce a global minimum of the dispersion curve at high-symmetry points $(0, 0)$, $(\frac{1}{2}, \frac{1}{2})$, $(\frac{1}{2}, 0)$ and along high-symmetry directions $[k, 0]$, $[k, k]$, $[\frac{1}{2}, k]$ and equivalent, Fig. 1(b). A condensation of a mode at one of the high-symmetry points leads to a low-symmetry commensurate phase. To produce an incommensurate modulation a condensation of one or two pairs of opposite wave vectors from the set of four equivalent wave vectors is required. Condensation of one pair leads to a stripe modulation. Condensation of two pairs of wave vectors would cause a two-dimensional quiltlike modulation $2q$. The $1q$ and $2q$ incommensurate or commensurate modulations are characterized by the wave-vector values which are usually close but not necessarily identical to the wave vector \mathbf{k} of the minimum of the dispersion curve. The difference comes from the influence of higher-order harmonics and/or additional umklapp terms, which cause the potential energy, Eqs. (1a)–(1c), to have a minimum at the wave vector different from the wave vector \mathbf{k} of the minimum of the dispersion curve.

III. GLOBAL PHASE DIAGRAM

The phase transition from normal phase to any of the low-symmetry commensurate or modulated phases is defined by vanishing of the value of the dispersion curve at the minimum, $\omega_{\min}^2(\mathbf{k}) = 0$, Eq. (7). The wave vector \mathbf{k} at the minimum of $\omega_{\min}^2(\mathbf{k})$ depends, of course, on the values of B and C potential parameters, and along a given direction is specified by the extremum condition which leads to

$$\cos 2\pi k = -\frac{B+2C}{4} \quad \text{along } [k, 0], \quad (8a)$$

$$\cos 2\pi k = -\frac{B}{4+2C} \quad \text{along } [k, k], \quad (8b)$$

$$\cos 2\pi k = -\frac{B-2C}{4} \quad \text{along } [\frac{1}{2}, k]. \quad (8c)$$

The corresponding values of the dispersion curves at the minima are

$$\omega_{\min}^2(k, 0) = A + 2B - \frac{(B+2C)^2}{4}, \quad (9a)$$

$$\omega_{\min}^2(k, k) = A - 4 - \frac{B^2}{2+C}, \quad (9b)$$

$$\omega_{\min}^2(\frac{1}{2}, k) = A - 2B - \frac{(B-2C)^2}{4}, \quad (9c)$$

respectively. The dispersion curve, Eq. (7), may have a minimum along one of the high-symmetry directions provided at least one of the conditions, Eqs. (8a)–(8c), is fulfilled. This imposes constraints on the B and C parameters because the $\cos 2\pi k$ has to be confined to the interval $[-1, 1]$. An analysis of Eqs. (8a)–(8c) brings us to a schematic global phase diagram of the square model, Fig. 2, in which only the general phases are indicated. Their stabilities are governed by the A parameter of the potential energy which should have such a value that the corresponding minimum of the dispersion curve $\omega_{\min}^2(\mathbf{k})$, Eqs. (9a)–(9c), takes a negative value. For all low-symmetry phases, the normal-symmetry–low-symmetry phase transition is given by the condition $\omega_{\min}^2(\mathbf{k}) = 0$. In Fig. 2 are shown three regions of stability of the commensurate phases $(0, 0)$, $(\frac{1}{2}, \frac{1}{2})$, $(\frac{1}{2}, 0)$, and regions of stability of modulated phases along $[k, 0]$, $[k, k]$, $[\frac{1}{2}, k]$ directions. The lines in Fig. 2 indicate approximate phase boundaries. In reality, depending on the value of the A parameter, the commensurate phases $(0, 0)$, $(\frac{1}{2}, \frac{1}{2})$, $(\frac{1}{2}, 0)$ will invade the regions of stability of modulated phases. Precisely, Fig. 2 represents the projection of the phase boundaries between different low-symmetry phases taken at the level of this A value which corresponds to the normal-symmetry–low-symmetry phase transition.

The harmonic part of the potential energy, Eq. (1b), allows us to specify the characteristic wave vector of the

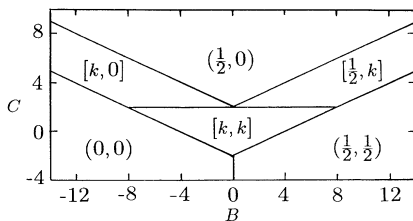


FIG. 2. Global phase diagram of the square-lattice model written in terms of B and C harmonic potential parameters, Eq. (1b).

low-symmetry phase, but cannot decide what dimensionality, $1q$ or $2q$, the modulation will have. The dimensionality of the modulation is defined by the fourth-order anharmonic term. From our numerical solutions we know that along the $[k, k]$ direction the modulation remains always of $1q$ type and that the stable $2q$ incommensurate modulations occur only along $[k, 0]$ and $[\frac{1}{2}, k]$ directions.

Consider then the free energy for the irreducible star of the $[k, 0]$ direction. Using Eq. (2), assuming that only the first modulation harmonic is taken into account, disregarding all lock-in terms, and counting the number of equivalent terms, one transforms the potential energy, Eqs. (1a)–(1c), to the form^{19,20}

$$F = 2\omega^2(k, 0) |Q_{k,0}|^2 + 2\omega^2(0, k) |Q_{0,k}|^2 + 3(1 + 4H \cos 2\pi k) (|Q_{k,0}|^4 + |Q_{0,k}|^4) + 12[1 + 2H(1 + \cos 4\pi k)] |Q_{k,0}|^2 |Q_{0,k}|^2. \quad (10)$$

The normal phase is defined by $|Q_{k,0}| = |Q_{0,k}| = 0$.

A single domain of the $1q$ incommensurate phase is defined by $|Q_{k,0}| \neq 0$ and $|Q_{0,k}| = 0$ and its potential energy, which follows from Eq. (10), after eliminating $|Q_{k,0}|$ through the extremum condition, becomes equal to

$$F_{1q} = -\frac{\omega^4}{3(1 + 4H \cos 2\pi k)}. \quad (11)$$

Similarly, for $2q$ incommensurate modulation, defined by equality of both modulation amplitudes $|Q_{k,0}| = |Q_{0,k}|$, the potential energy takes the form

$$F_{2q} = -\frac{\omega^4}{\frac{9}{2} + 6H(1 + \cos 2\pi k + \cos 4\pi k)}. \quad (12)$$

The expressions, Eqs. (10)–(12), impose restrictions on the coefficient H of the anharmonic term. Namely, the $1q$ incommensurate phase along the $[k, 0]$ direction is stable, if

$$H > -\frac{1}{4 \cos 2\pi k} \quad (13)$$

and the $2q$ modulation remains stable provided

$$H > -\frac{3}{4(1 + \cos 2\pi k + \cos 4\pi k)}. \quad (14)$$

A comparison of the free energies for $1q$ and $2q$ modulated phases, Eqs. (11)–(12), allows us to establish that the $2q$ phase is more stable than the $1q$ one, if

$$H < -\frac{1}{4(1 - \cos 2\pi k + \cos 4\pi k)}. \quad (15)$$

Making use of inequalities Eqs. (13)–(15) we draw in Fig. 3 part of the phase diagram. It shows in the space of the wave vector k of the minimum of the dispersion curve and the anharmonic coefficient H , where the $1q$ and $2q$ modulated phases are stable, and where the whole system becomes unstable. The wave vector k is related with B and C parameters for modulations along $[k, 0]$ and $[\frac{1}{2}, k]$, by Eq. (8a) or (8c), respectively. Remarkable is that $2q$ modulation is stable only below a critical value of coeffi-

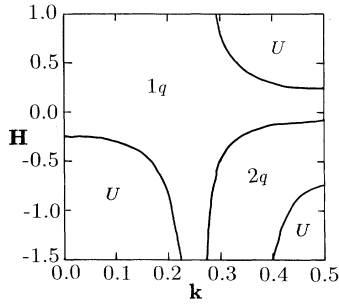


FIG. 3. Section of the phase diagram of the square-lattice model written in terms of H anharmonic potential parameter, Eq. (1c), and the wave vector k of the minimum of the dispersion curve, Eq. (7), for $[k, 0]$ (and $[\frac{1}{2}, \frac{1}{2} - k]$) directions. It shows the regions of stability of $1q$ and $2q$ modulated phases and regions where the system is unstable (U).

cient $H < -\frac{1}{12}$, and for the wave vectors $k > 0.25$. Close to zone center the modulation remains always of $1q$ type.

IV. NUMERICAL METHOD

The ground state of the square-lattice model depends on A, B, C , and H potential parameters. Some sections of the phase diagram of the model have been found numerically by minimizing the potential energy, Eqs. (1a)–(1c), using the gradient method.²¹ The minimization process for $2q$ phases has been performed on the crystallites of $M \times M$ or $2M \times 2M$ lattice constants, for modulations characterized by the wave vectors $(k, 0)$, $(0, k)$ and $(\frac{1}{2}, k)$, $(-k, \frac{1}{2})$, respectively. For $2q$ modulation directed along (k, k) , $(k, -k)$, the procedure was different. The model has been treated as a new face-centered-square lattice with two particles per unit cell and with new lattice vectors $\mathbf{a}' = \mathbf{a} + \mathbf{b}$ and $\mathbf{b}' = \mathbf{a} - \mathbf{b}$. The minimized

block had a size of $M' \times M'$ unit cells.

A commensurate modulation characterized either by the wave vectors $k_x = (N/M)\mathbf{a}^*$, $k_y = (N/M)\mathbf{b}^*$ or $k_{x'} = (N/M)\mathbf{a}'^*$, $k_{y'} = (N/M)\mathbf{b}'^*$, respectively, where N and M are integers, fitted to the selected crystallites $M \times M$, $2M \times 2M$, or $M' \times M'$, on which periodic boundary conditions were imposed. The minimization procedure started from initial conditions taken in the form of two cosine waves of particle displacements directed along \mathbf{a}^* , \mathbf{b}^* or \mathbf{a}'^* , \mathbf{b}'^* , respectively. The wave vector of the initial modulation has been taken to be equal to N/M . We have limited the N and M integers to $N = 0, 1, \dots, 11$ and $M = 1, 2, \dots, 21$, and admitted only fractions N/M which fall into the interval $[0, \frac{1}{2}]$. Phases $N/M = \frac{0}{1}, \frac{1}{2}, \frac{1}{3}, \frac{1}{4}, \frac{1}{5}, \frac{1}{6}$, if stable in sufficiently wide interval, are called commensurate. The remaining high-order commensurate phases were treated as incommensurate ones. This is the usual practical approach, since anyway their stability intervals, in terms of potential parameters, were negligible. Moreover, at finite temperatures the thermal fluctuations would destroy the weakly locked high-order commensurate phases, giving in result a state with incommensurate modulation.

The $1q$ modulated phases have been treated in a similar way as the $2q$ phases. The only difference was that the crystallites $M \times M$, $2M \times 2M$, and $M' \times M'$ have been reduced to chains $M \times 1$, $2M \times 2$, and $M' \times 1$, and that the initial conditions were taken in the form of a single cosine wave directed along the modulation.

V. DETAILED PHASE DIAGRAMS

Even at $T = 0$, the modulated phases exist only in part of (A, B, C, H) space. In particular, the B and C parameters must fall into the regions indicated in Fig. 2. Values of B and C parameters decide whether the modulation is directed along $[k, 0]$, $[\frac{1}{2}, k]$, $[k, k]$ or the phase

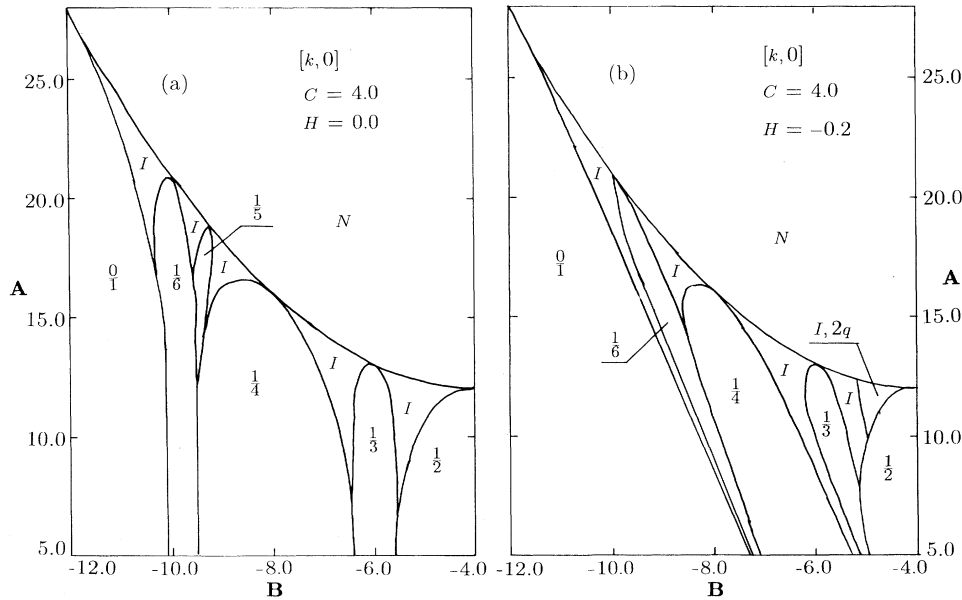


FIG. 4. Phase diagrams of the square-lattice model ($C = 4.0$) for modulated phases along $[k, 0]$ (and $[\frac{1}{2}, \frac{1}{2} - k]$) direction and for anharmonic parameters: (a) $H = 0.0$ and (b) $H = -0.2$. N and I denote normal and incommensurate phases, respectively. All phases are $1q$, except those denoted $2q$.

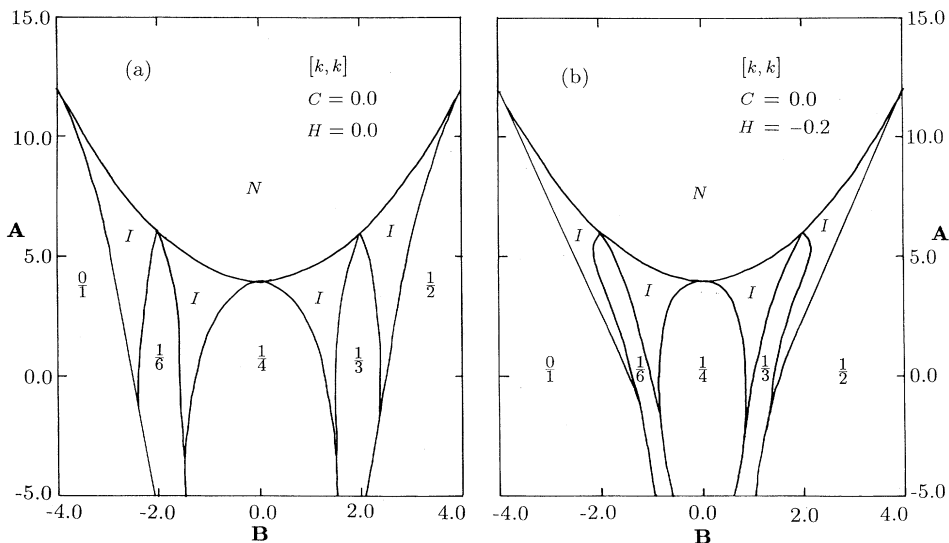


FIG. 5. Phase diagrams of the square-lattice model ($C = 0.0$) for modulated phases along $[k, k]$ direction and for anharmonic parameters: (a) $H = 0.0$ and (b) $H = -0.2$. N and I denote normal and incommensurate phases, respectively. All phases are $1q$.

remains commensurate. Moreover, phases characterized by the modulation wave vectors rotated away from the above high-symmetry directions proved to be unstable.

Some sections of the phase diagram are presented in Figs. 4 and 5. The figures show phase diagrams for $C = 4.0$ and 0.0 and $H = 0.0$ and -0.2 . Figures 4 and 5 correspond to modulated phases along $[k, 0]$ and $[k, k]$, respectively. The phase diagram along $[k, 0]$, Fig. 4, can be identified with the phase diagram describing modulated phases along $[\frac{1}{2}, \frac{1}{2} - k]$, provided one changes $B \rightarrow -B$,

Eqs. (4) and (5). For example, the commensurate phase $\frac{1}{6}$ along $[k, 0]$ becomes $(\frac{1}{2}, \frac{1}{3})$ along $[\frac{1}{2}, k]$.

In the phase diagrams, Figs. 4 and 5, one sees regions of commensurate and incommensurate phases, and the most interesting features appear close to the phase boundary to the normal phase. Commensurate phases with modulation wave vectors $0, \frac{1}{6}, \frac{1}{5}, \frac{1}{4}, \frac{1}{3}$, and $\frac{1}{2}$ cover large areas of the phase diagrams. In between are placed incommensurate phases.

The phase diagram with modulated phases along the $[k, k]$ direction, Fig. 5, is symmetric with respect to the point $(\frac{1}{4}, \frac{1}{4})$. It is a consequence of the relation (5). Along the $[k, k]$ direction one observes the $1q$ modulated phases only.

At $H = 0$ the phase diagram along the $[k, 0]$ direction possesses $1q$ modulated phases only. At $H < 0$, the phase boundaries change the slope, consequently the region of stability of commensurate phase characterized by the wave vector $k = 0$ increases and the region of stability of remaining high-order commensurate phases decreases. The commensurate phase $\frac{1}{5}$ squeezes so much that it disappears. The $2q$ phase appears close to the Brillouin zone. When H decreases further the phase boundary between incommensurate phases $1q$ and $2q$ shifts towards the $(\frac{1}{4}, 0)$ wave vector. This behavior is clearly seen in Fig. 6, which shows part of the phase diagram for decreasing values of H . There are neighboring regions of $1q$ and $2q$ incommensurate phases, and regions of $1q$ and $2q$ commensurate phases $\frac{1}{3}$. However, the commensurate phase $\frac{1}{2}$ becomes $2q$ modulated only at very negative values of H , Fig. 6d.

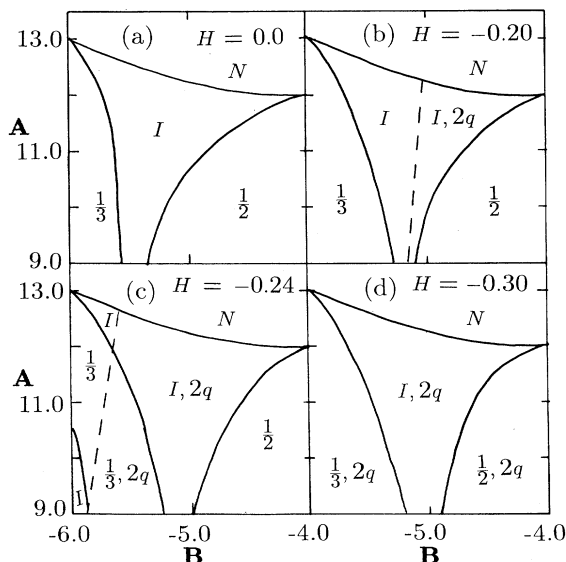


FIG. 6. Part of the phase diagram of the square-lattice model ($C = 4.0$) for modulated phases along $[k, 0]$ (and $[\frac{1}{2}, \frac{1}{2} - k]$) direction and for anharmonic parameters: (a) $H = 0.0$, (b) $H = -0.20$, (c) $H = -0.24$, and (d) $H = -0.30$. N and I denote normal and incommensurate phases, respectively. All phases are $1q$ except those denoted $2q$. Dotted line is the phase boundary between $1q$ and $2q$ regions.

VI. FINAL REMARKS

The calculated phase diagrams of the square-lattice model correspond to their ground states. This model can be considered as a selection of these degrees of freedom of a real crystal, which are responsible for the formation of commensurate and incommensurate modulations. The modifications of the phase diagram at finite tem-

perature can be found in mean field approximation,^{22,23} in which the parameters A, B, C are renormalized and become slightly temperature dependent. This approach, however, might underestimate the renormalization, since it does not take into account fluctuations of other degrees of freedom not considered explicitly in our model.

A remarkable feature of the square-lattice model is that the stability of the $2q$ modulated phase is caused by the fourth-order anharmonic interaction. Absence of this interaction involves $1q$ commensurate and incommensurate modulations in the entire phase diagram. This nonlocal anharmonic force is present only if the potential energy has a three-body character. Indeed, such an interaction is needed to stabilize the nodes of two crossing modulated waves. Moreover, the stability of the $2q$ modulated phase

is achieved only then, if the magnitude of the mentioned anharmonic term exceeds a critical value. It is quite possible that the nature of crystals does not supply potentials which fulfill this criterion. That might be one of the reasons that $2q$ modulated phases are experimentally observed so rarely.

ACKNOWLEDGMENTS

The author would like to thank H. Warhanek, W. Schranz, A. Fuith, and H. Kabelka for discussions and fruitful comments made during his visit at the Institut für Experimentalphysik der Universität Wien. This work was fully supported by the State Committee of Scientific Research (KBN), Grant No. 2 0183 91 01.

-
- ¹H. Z. Cummins, Phys. Rep. **185**, 211 (1990).
²W. Selke, Phys. Rep. **170**, 213 (1988).
³S. Barré, H. Mutka, C. Roucau, A. Litzler, J. Schneck, J.C. Tolédano, S. Bouffard, and F. Rullier-Albenque, Phys. Rev. B **43**, 11 154 (1991).
⁴J.C. Tolédano and P. Tolédano, *Landau Theory of Phase Transitions* (World-Scientific, Singapore, 1987).
⁵S. Barré, H. Mutka, and C. Roucau, Phys. Rev. B **38**, 9113 (1988).
⁶D. Broddin, G. Van Tendeloo, J. Van Landuyt, S. Amelinckx, R. Portier, M. Guymont, and A. Loiseau, Philos. Mag. A **54**, 395 (1986).
⁷D. Broddin, G. Van Tendeloo, J. Van Landuyt, and S. Amelinckx, Philos. Mag. A **59**, 47 (1989).
⁸J. Bohr, D. Broddin, and A. Loiseau, Phys. Rev. B **42**, 1052 (1990).
⁹G. Dolino, in *Incommensurate Phases in Dielectrics*, Modern Problems in Condensed Matter Sciences Vol. 14, edited by R. Blinc and A.P. Levanyuk (North-Holland, Amsterdam, 1986).
¹⁰Shun-ichiro Koh and Yasusada Yamada, J. Phys. Soc. Jpn. **56**, 1794 (1987).
¹¹E. Snoeck, C. Roucau, and P. Saint-Gregoire, J. Phys. (Paris) **47**, 2041 (1986).
¹²K.K. Fung, S. McKernan, J.W. Steed, and J.A. Wilson, J. Phys. C **14**, 5417 (1981).
¹³J. Van Landuyt, Physica B **99**, 12 (1980).
¹⁴A. Joets and R. Ribotta, J. Phys. (Paris) **47**, 595 (1986).
¹⁵W. Selke, K. Binder, and W. Kinzel, Surf. Sci. **125**, 74 (1983).
¹⁶D.P. Landau and K. Binder, Phys. Rev. B **31**, 5946 (1985).
¹⁷M.J. Velgakis and J. Oitamaa, J. Phys. A **21**, 547 (1988).
¹⁸K. Parlinski, S. Kwiecinski, and A. Urbanski, Phys. Rev. B **46**, 5110 (1992).
¹⁹K. Parlinski and K.H. Michel, Phys. Rev. B **39**, 396 (1984).
²⁰K. Parlinski and F. Dénoyer, Phys. Rev. B **41**, 11 428 (1990).
²¹K. Parlinski, Comput. Phys. Rep. **8**, 153 (1988).
²²T. Janssen and J.A. Tjon, Phys. Rev. B **25**, 2245 (1981).
²³J.J.M. Slot and T. Janssen, Physica D **32**, 27 (1988).